Kinetic roughening with anisotropic growth rules

Raffaele Cafiero
Laboratoire de Physique et Méchanique des Milieux Héterogenes, Ecole Supérieure de Physique et de Chimie Industrielles, 10, rue Vauquelin, 75231 Paris Cedex 05, France

(Received 13 September 2000; revised manuscript received 17 October 2000; published 27 March 2001)

Inspired by the chemical etching processes, where experiments show that growth rates depending on the local environment might play a fundamental role in determining the properties of the etched surfaces, we study here a model for kinetic roughening that includes explicitly an anisotropic effect in the growth rules. Our model introduces a dependence of the growth rules on the local environment conditions, i.e., on the local curvature of the surface. Variables with different local curvatures of the surface, in fact, present different quenched disorder and a parameter p (which could represent different experimental conditions) is introduced to account for different time scales for the different classes of variables. We show that the introduction of this *time scale separation* in the model leads to a crossover effect on the roughness properties. This effect could explain the scattering in the experimental measurements available in the literature. The interplay between anisotropy and the crossover effect and the dependence of critical properties on parameter p is investigated as well as the relationship with the known universality classes.

DOI: 10.1103/PhysRevE.63.046108 PACS number(s): 05.65.+b, 68.35.Ja, 81.65.Cf

I. INTRODUCTION

In the last few years the study of physical phenomena characterized by a degree of self-organization [1], has attracted a lot of interest. These models are usually cellular automata models defined on a discretized lattice, with a growth rule that can be either stochastic, when the inhomogeneities in the system change with a time scale smaller than the characteristic time scale of the dynamical evolution (noise), or deterministic with a quenched disorder, which accounts for the effect of inhomogeneities inside a solid medium. Both kinds of dynamical rules are characterized by an evolution towards an attractive fixed point in which scale free fluctuations in time and space are present [2].

The problem of kinetic roughening belongs to this class of models. It received recently an increasing interest in relation with nonequilibrium growth models [3] and in view of its practical applications: chemical vapor deposition [4] and electrochemical deposition [5] are just two examples.

In this perspective, one is interested in identifying the dynamic universality classes of kinetic roughening processes and several models has been defined starting from the models falling in the universality class of the Kardar-Parisi-Zhang (KPZ) equation [6]. This equation describes the properties of an interface $h(x,t)$ driven by a stochastic noise and gives a roughness exponent $\chi=0.5$. Other models are more suitable to describe the propagation of interfaces in random media, i.e., with a quenched disorder. These models are driven by an extremal dynamics. In this class fall the so-called Sneppen model [7] (referred to as model B) and the pinning model by directed percolation [8], which predict a roughness exponent equal to $\chi=0.63$. These models produce self-affine surfaces. Recently, a model has been introduced to describe some etching experiments, which leads to the formation of self-similar (fractal) structures, and which has been shown to fall in the percolation universality class [9]. Many experiments on surface roughening [10–12], however, as well as experiments on chemical etching [13] produce self-affine surfaces instead of self-similar ones. In this paper, we will focus on kinetic roughening phenomena leading to *self-affine* ($\chi<1$) surfaces.

We recall that the roughness exponent is defined by the ensemble-averaged width of the interface as $W(l,t)=\langle[h(x,t)-\langle h(x,t)\rangle]^2\rangle^{1/2}\sim l^{\chi}f(t^{1/z}/l)$, where z is the so-called dynamical exponent, the angular brackets denote the average over all segments of the interface of length l and over all different realizations. f is a scaling function such that $f(y)\sim y^{\chi}$ for $y\ll 1$ and $f(y)=\text{const}$ for $y\gg 1$. The exponent $\beta=\chi/z$ describes the transient roughening, during which the surface evolves from the initial condition toward the final self-affine structure.

In spite of the strong universality exhibited by the KPZ and Sneppen models, in many experimental studies one measures values of χ that are above the ones predicted by both the KPZ and Sneppen universality classes. To give some examples, we remember the experimental studies of paper burning for which one gets $\chi=0.70\pm0.03$ [10], or the propagation of a forced fluid front in a porous medium, which exhibits a roughness exponent $\chi=0.73\pm0.03$ [11] and $\chi=0.88\pm0.08$ [12].

In this paper we propose a generalized model for kinetic roughening characterized by anisotropic growth rules and, as a consequence, separated time scales for the dynamics. The existence of this time-scale separation induces a cross-over effect in the roughness properties, which could erroneously appear as a genuine nonuniversal critical behavior, and could give an explanation for the above cited scattered experimental results.

Some results presented here have been already briefly reported on in a letter [13]. In this long paper we give a detailed, complete description of our previous work. Moreover, we present a set of new numerical results, which allow us to reach different and better founded conclusions with respect to Ref. [13].

The idea underlying the model is that some experimental parameters can introduce a characteristic scale in the system,

separating different scaling behaviors. In particular we consider a model that includes explicitly an anisotropy factor, say a growth rule dependent on the local environment of the growing site. The model thus presents a complex interplay between a global equilibrium and the conditions of a local dynamics. This choice is motivated by the observation of roughening phenomena occurring in etching processes that represent an important tool either in academic research or in device technology. Their importance is related to the preparation of single-crystal samples of desired dimensions, shapes, and orientations. Etching is usually applied to obtain desired mesas and grooves in semiconductor wafers and multilayers [14].

In the same field, although in a different context, etching processes are used to produce textured optical sheets, which allow to exploit the light trapping by total internal reflection to increase the effective absorption in the indirect-gap semiconductors crystalline silicon. Light trapping, originally suggested to increase the response speed of silicon photodiodes while maintaining high quantum efficiency in the near infrared, was later indicated as an important benefit for solar cells [14].

The general suffix *etching* indicates the ensemble of operations that involve the removal of materials by expending energy either by mechanical, thermal, or chemical means. In Ref. [13] the authors focused their attention on chemical etching processes as a reference point to formulate the model. One of the most important properties of these processes is represented by the intrinsic anisotropy [15,16] of the etch rates. For instance in samples of crystalline silicon etched in solutions of aqueous potassium hydroxide (K-OH) with isopropil alcohol, depending on the concentration of the etchant and the temperature, the (111) direction etches slower than the others by a factor that can be of order 100 or more [17]. The degree of anisotropy affects the properties of the surface, which turns out to be rough with an apparently nonuniversal roughness exponent.

Although the definition of the model is very general we will briefly consider the chemistry of the etching process in order to exhibit a physical framework that allows to understand the meaning of the definitions and their interpretation.

The disorder in the etching process is related to the impurities in the lattice. Such impurities, e.g., vacant atoms, reduce the binding energy of atoms nearby the vacancy. By assigning to each site (atom) of our lattice a random number x_i we assume that a distribution of vacancies, or other kinds of impurities, is present in the system, and this induces fluctuations in the binding energy of atoms due to this disorder. If we assume to be in a condition of slow dynamics, that is to say the driving field (which in our case is represented by the concentration of etchant) tends to zero [18], we can look at the etching as an extremal process, where the etchant dissolves the atom with the smallest binding energy. This is correct for low etchant concentrations and corresponds actually to the situation experimentally more interesting, in which rough surfaces are produced.

In order to reproduce the experimental conditions (type of etchant, concentration, temperature) a microscopic model for the physical process should contain some tunable parameters

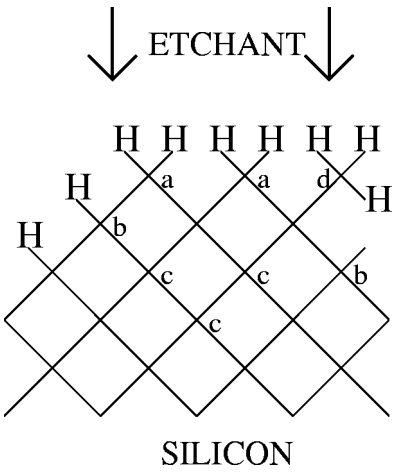

FIG. 1. Schematic representation of the crystalline silicon lattice as a square lattice.

(at least one). In our model, the anisotropy is introduced by a phenomenological tunable parameter p, which distinguishes sites with a different local environment.

The introduction of the parameter p defines a characteristic scale in the problem. As a result the critical properties of the model are characterized by a continuous crossover between two universality classes corresponding to the roughness exponents $\chi=1$ and $\chi=0.63$ (Sneppen models *A* and *B*, respectively [7]). In particular one can define a parameter $r=p/1-p$, which measures the time-scale separation between the dynamics of the different classes of sites. For lengths $l>l^*\propto 1/2-p/p$ one observes a behavior characteristic of the Sneppen model *B* universality class ($\chi=0.63$), while for $l<l^*\propto 1/2-p/p$ one observes a behavior characteristic of the Sneppen model *A* universality class. The existence of this crossover is difficult to detect directly on the plot for the scaling of the surface width $W^2(l)$ (especially for finite sets of data) and it becomes evident looking at the power spectra. This explains why large-scale experiments could give the impression of nonuniversality in the critical properties of rough surfaces.

Let us look at the meaning of p in the case of etching. If we represent the crystalline lattice of the silicon on a two-dimensional plane we can imagine a square lattice where (see Fig. 1) the atoms can be found in each of the four positions marked in figure by the letters a–d. The four positions correspond to different oxidation states: from the situation (c) (oxidation number 0) which occurs only in the bulk, to the situation (d) (oxidation number -3). Note that all the surface atoms are passivated by hydrogen atoms. The atoms in the positions (a) and (b), corresponding, respectively, to the oxidation numbers -2 and -1 (two and one heteropolar bonds, i.e., Si-H bonds), play an important role in explaining, at least from a heuristic point of view, the origin of the anisotropy in the etched rates [16]. The parameter p quantifies the ratio of the etch rates between the sites in the positions (a) and (b). The basic idea is that in the (111) plane of silicon, there is only one heteropolar bond per silicon atom. Therefore there are three bonds to break for dissolution, while other planes [except the (110)] have more than one

heteropolar bond and accordingly a smaller number of bonds must be broken.

The paper is organized as follows. In Sec. II we describe in detail the model and the set up of numerical simulations. In Sec. III we present and discuss the numerical results in relation with the Sneppen model A and B universality classes. In Sec. IV a discussion of the results and some conclusions are drawn together with a planning of future researches.

II. MODEL

We give now a detailed definition of the model. The model is defined on a square 2D lattice tilted at 45° (see Fig. 1). We consider a $1+1$ dimensional interface $h(x)=h(x,t)$ with $x=1,2,\ldots,L$, where L is the linear extension of the interface in the x direction. The initial condition for the dynamical evolution of this interface is given by $h(2x,0)=1\ \forall x\in[1,L/2]$ and $h(2x-1,0)=0\ \forall x\in[1,L/2]$, in order to have both classes of variables (lattice planes) participating in the dynamics from the beginning, but different initial conditions do not change the properties of the model. The interface, which satisfies locally the conditions [19]

$$\begin{aligned} &|h(x,t)+1-h(x-1,t)|\leqslant 1,\\ &|h(x,t)+1-h(x+1,t)|\leqslant 1 \end{aligned} \tag{1}$$

contains two classes of random variables that correspond to two separate classes of sites. The sites (M) for which it holds $\nabla^2 h>0$ (called minimum sites) which are, microscopically, the atoms with two heteropolar bonds, and the sites on a slope [slope (S) sites] for which one has $\nabla^2 h=0$. These last sites correspond microscopically to atoms with one heteropolar bond. To each class of sites is assigned a class of Gaussian distributed uncorrelated random variables that mimic the disorder, and represents physically, for the case of etching, the binding energy of atoms:

$$\eta(x,h)\in\begin{cases}[0{:}0.5] & \text{if } x \text{ is such that } \nabla^2 h=0\\ (0.5{:}1] & \text{if } x \text{ is such that } \nabla^2 h>0.\end{cases} \tag{2}$$

The sites with $\nabla^2 h<0$, for which all the chemical bonds are homopolar, i.e., Si-Si, do not take part to the dynamics and they have assigned a zero value of the random variable. Periodic boundary conditions are assumed along the x direction.

The system evolves by updating the site i^* with the largest random variable in one of the two classes of sites chosen, at its turn, with a probability p. One thus updates with probability p a site (S) and with probability $1-p$ a site (M) according to the rules (see Fig. 2):

(1) $h(i^*,t+1)=h(i^*,t)+2,\ \eta[i^*,h(i^*,t+1),t+1]=0$,

(2) updating all the sites necessary to make satisfied the conditions 1 (this phase is assumed to be instantaneous with respect to extremal dynamics),

(3) updating of the random variables for the sites, which changed their class of belonging. In particular $\eta(x,h,t+1)=1/2*RAN$ if $\eta(x,h,t)=0$ and $\eta(x,h,t+1)=\eta(x,h,t)+1/2$ if $\eta(x,h,t)\neq 0$, where RAN is a random value between 0 and 1,

(4) updating of the random variables of the sites, which have changed their height but that did not change their class of belonging, (sites S only): $\eta(x,h,t+1)=1/2*RAN$.

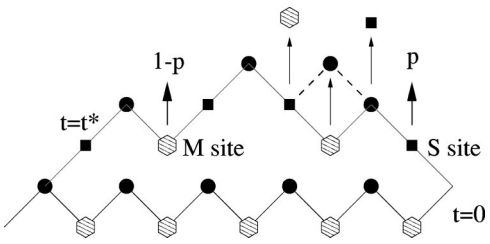

FIG. 2. Schematic representation of interface dynamics.

The parameter p can vary in the range $[0{:}1/2]$. If we define t_S as the characteristic time scale for S variables and t_M the characteristic time scale for M variables one has

$$r=\frac{t_M}{t_S}=\frac{p}{1-p}. \tag{3}$$

The growth of the interface, in the etching process, represents the invasion of the etchants into the silicon wafer. From this point of view the updating of the sites (S) mimics the etching of the (111) planes and the updating of the (M) sites the etching in the (100) direction. For $p=1/2$ all the sites which take part in the dynamics are equivalent and there is no anisotropy ($r=1$), whereas the case $p=0$ corresponds to the maximal anisotropy in which $v_{(111)}/v_{(100)}=r=0$, where $v_{(111)}$ and $v_{(100)}$ are the etch rates in the corresponding directions.

Our model can be viewed as a variation of the Sneppen model for quenched surface growth, where two important elements are added: (1) The anisotropy in the distribution of the quenched random field, depending on the local characteristics of the growing surface and (2) a time-scale separation for the dynamical evolution of the two classes of variables (S sites and M sites), which is tuned by the parameter p.

III. NUMERICAL RESULTS

We have studied this cellular automata by numerical simulations in order to analyze its dynamical roughening properties. The sizes we have chosen for the numerical simulations range from $L=2048$ to $L=8192$. For each value of p (we have considered $p=0.0,0.02,0.2,0.5$), 10^2 simulations lasting 10^7 time steps have been performed and we have computed the growth exponent β, which rules the time evolution of the width $W(t)$ of the surface [$W(t)\sim t^{\beta}$] before the stationary state is reached, and the roughness exponent χ, which gives the scaling of the width of the surface [$W(l)\sim l^{\chi}$], in the stationary state. The stationary state is called self-organized in that it is reached spontaneously by the system independently of the initial conditions. This self-organization is confirmed by an analysis of the temporal evolution of the distribution of quenched variables [the

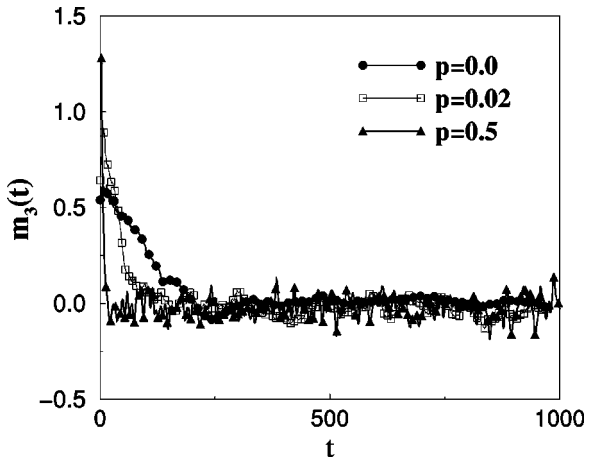

FIG. 3. Time evolution (adimensional units) of the moment m_3 (adimensional units) of the growing interface, normalized by the second moment, for $p=0.0$, 0.02, and 0.5 (skewness). One sees that asymptotically m_3 vanishes for all values of p.

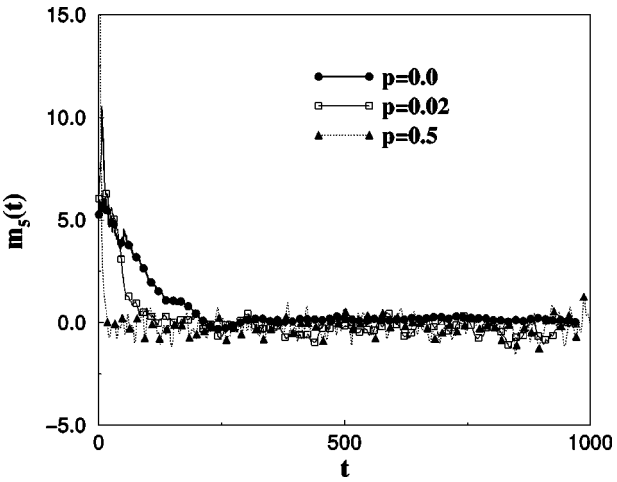

FIG. 5. Time evolution (adimensional units) of the moment m_5 (adimensional units) of the growing interface, normalized by the second moment, for $p=0.0$, 0.02, and 0.5. One sees that asymptotically m_5 vanishes for all values of p.

histogram $\Phi_t(\eta)$]. To characterize temporal correlations in the dynamics and check that the asymptotic state is critical, we studied the distribution of the avalanches in the asymptotic state. As an independent check about the universality of the roughness properties of the model, we have studied numerically the power spectrum $S(k)$ of the height profile.

To ensure that the system is in the stationary state, we studied the behavior of the nth moments (for $n=3,4,5$) of $h(x,t)$ normalized to second momentum:

$$m_n(t)=\frac{\left\langle \sum_i [h(i,t)-\overline{h}(t)]^n \right\rangle}{\left(\left\langle \sum_i [h(i,t)-\overline{h}(t)]^2 \right\rangle \right)^{n/2}}, \tag{4}$$

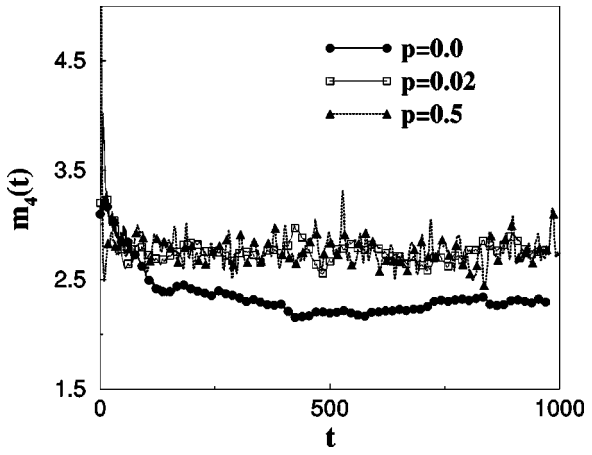

FIG. 4. Time evolution (adimensional units) of the moment m_4 (adimensional units) of the growing interface, normalized by the second moment, for $p=0.0$, 0.02, and 0.5. One sees that asymptotically m_4 tends to different constant values for the different values of p.

where $\overline{h}(t)$ is the mean surface height at time t. We get that, after a transient, all the odd moments vanish and the even ones tend to constant values (see Figs. 3–5). In particular the condition for the skewness $m_3=0$ (Fig. 3), which characterizes the stationary critical state [7], is realized after about 10^3 time steps per site, independent of the value of p. These results imply that the higher moments of the variable $h(x,t)-\langle h\rangle$ scale in a trivial way (they are powers of the second moment), and after the transient the probability distribution of the variable $h(x,t)$, which can be viewed as a random variable, is Gaussian. The amplitude of the normalized even moments m_{2n}, in the asymptotic stationary state, characterizes the roughness properties of the interface.

In Table I we report the measured values for the dynamical exponents β, which turns out to be independent of p. Figures 6–9 show the scaling behavior of $W^2(l)$ for different values of p. For $p=0.0$ (i.e., maximal anisotropy) the measured values of χ are affected by a finite-size effect and they tend, in the limit $L\to\infty$, to the value $\chi=1.0$ found for Sneppen model A [7] (Fig. 6). In this case the surface is composed by very big pyramids (Fig. 10). On the other hand, for $p=0.5$, one recovers the universality class of Sneppen model B with $\chi=0.63$ (Fig. 9). For all the other values of p between 0 and 0.5 ($p=0.02$ in Fig. 7 and $p=0.2$ in Fig. 8), trying to perform fits away from the saturation regions, one would be tempted to invoke the existence of a nonuniversal behavior ruled by the parameter p. A careful observation

TABLE I. Values of the dynamical exponent β in our model for different values of the anisotropy parameter p.

p	β
0.0	0.96(2)
0.02	0.95(2)
0.2	0.94(2)
0.5	0.95(2)

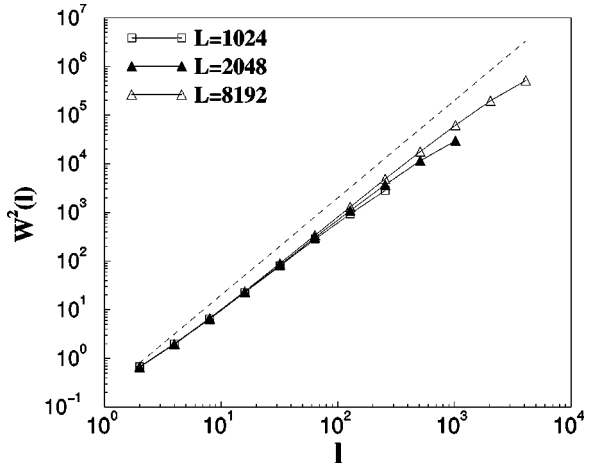

FIG. 6. $W^2(l)$ vs l [both $W^2(l)$ and l are expressed in adimensional units] for $p=0.0$ and different system sizes. The lower fit (dot-dashed line) corresponds to a size $L=512$, giving and exponent $\chi=0.88(2)$, while the upper fit (dashed line) corresponds to a size $L=8192$ and gives an exponent $\chi=0.96(2)$. In this case we expect that the exponent converges to $\chi=1$ in the limit $L\to\infty$.

puts in evidence that the curves for $W^2(l)$ seem to exhibit a crossover between the Sneppen models *A* and *B* universality classes. On the basis of p one can define a characteristic length $l^*\propto 1/2-p/p$ above which one could see the $\chi=0.63$ behavior and below which one could see the $\chi=1$ behavior. We shall come back to these considerations later on when we shall discuss the power spectra.

We have also studied the time evolution of the distribution of random variables on the invading interface [the histogram $\Phi_t(\eta)$, where η is a generic value for $\eta(x,h)$], which is of great importance for models with extremal dynamics. The results of the simulation are shown in Figs. 11–14. One can see that $\Phi_t(\eta)$ self-organizes, for $p\neq 0$, after about 10^5 time steps, into a distribution that is the superposition of two theta functions, one for each class of variables, each one characterized by a critical threshold $p_c(p)$ depending on the parameter p. The meaning of these thresholds is that only *S* variables larger than η_c^S and *M* variables

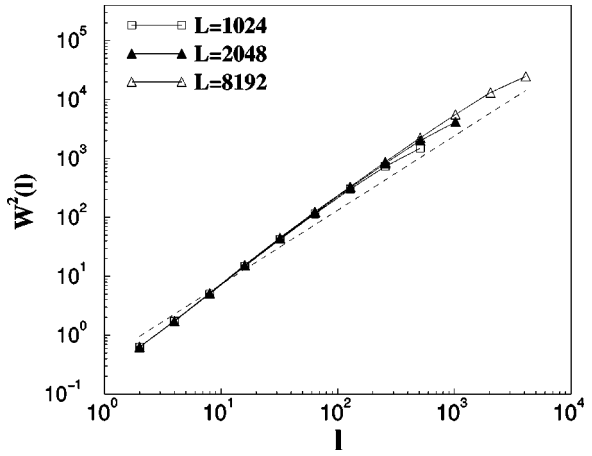

FIG. 7. $W^2(l)$ vs l [both $W^2(l)$ and l are expressed in adimensional units] for $p=0.02$ and different system sizes.

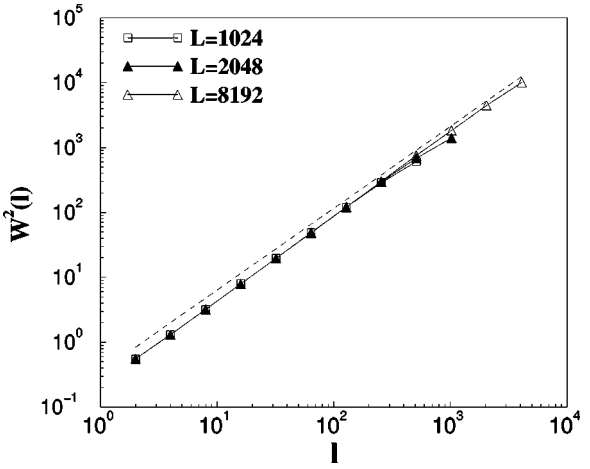

FIG. 8. $W^2(l)$ vs l [both $W^2(l)$ and l are expressed in adimensional units] for $p=0.2$ and different system sizes.

larger than η_c^M can grow [2]. For $p=0$, instead, the histogram has no self-organized critical state (Fig. 11). Looking carefully at Fig. 11 we can see that, while in the initial transient there are a few *S* sites, in the asymptotic state most sites are *S* sites. In fact nearly all variables larger than 0.5 (the *M* variables) are disappeared. This observation agrees with the actual structure of the surface, which is composed by very big pyramids (Fig. 10), with a roughness exponent $\chi\simeq 1$. This picture is confirmed by the acceptance profile $a(\eta)$, which is shown in Fig. 15. As in the Bak and Sneppen (BS) model, the acceptation profile (that is to say the distribution of the values of all updated quenched variables up to the actual time) exhibits correlation properties (it is not flat), reflecting temporal correlations in the dynamics. But, while the acceptation profile for *S* variables is quite similar to that of the BS model, going to zero linearly at p_c, the acceptation profile for *M* variables has a more complicated behavior. This difference originates maybe from the fact that *S* variables ($\eta\in[0.5,1]$) can turn into *M* ($\eta\in[0,0.5]$) variables during the dynamics of the system, while *M* variables cannot become *S* variables. Moreover, *S* variables can have devel-

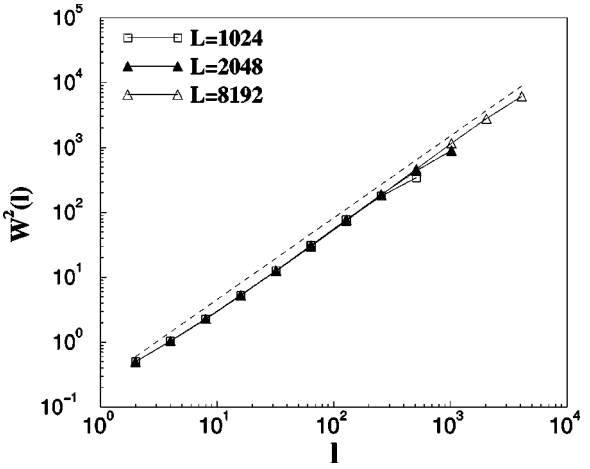

FIG. 9. $W^2(l)$ vs l [both $W^2(l)$ and l are expressed in adimensional units] for $p=0.5$ and different system sizes.

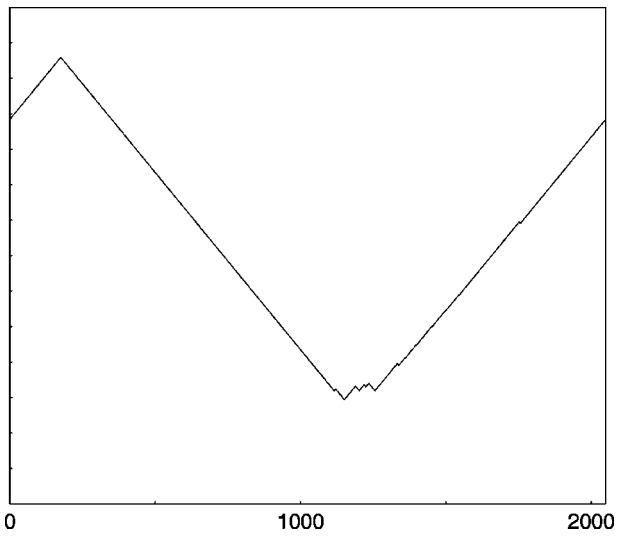

FIG. 10. A realization of the growing surface for $p=0.0$ (horizontal adimensional position on the x axis). The surface is composed by very big pyramids, thus with a strong prevalence of S sites.

oped correlations before the transition to M variable and this affects the shape of $a(\eta)$ for $\eta \in [0.5,1]$. This might account for the linear part of the acceptation profile of M variables, around $\eta=1$, but the nonlinear part is more puzzling. The coupling between S variables and m variables could play a role in this behavior, too, but at the moment we have no clear explanation of it. From the $a(\eta)$ we can get a good estimation of the critical thresholds η_c^S and η_c^M for different values of p (see Table II).

The stationary state is characterized by a constant ratio between S and M sites, that is to say the evolution equation for the densities ρ_S and ρ_M of sites S and M, respectively, have an attractive fixed point in the stationary state [see Figs. 16(a)–16(d)], with the asymptotic values of ρ_S, ρ_M depending on the parameter p. One interesting observation is that, even in the case $p=0$, that is to say only M sites can be selected by the extremal dynamical rule, there is a stationary state for the system with $\rho_S \neq 0$. This is due to the particular geometry of the lattice, for which the growth of an M site implies the creation or annihilation of some S sites. In other words, there cannot be surfaces without slopes (S sites).

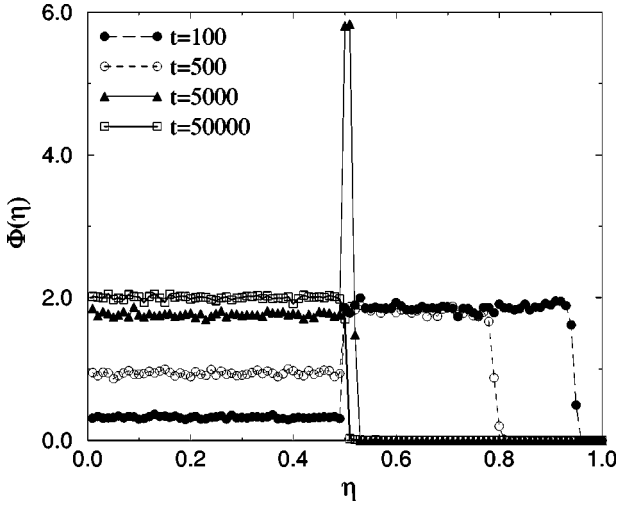

FIG. 11. Histogram $\Phi(\eta)$ (η is an adimensional number) of quenched variables, at different times t (adimensional computer units), for $p=0.0$. Asymptotically, all (most of the) M variables are eliminated.

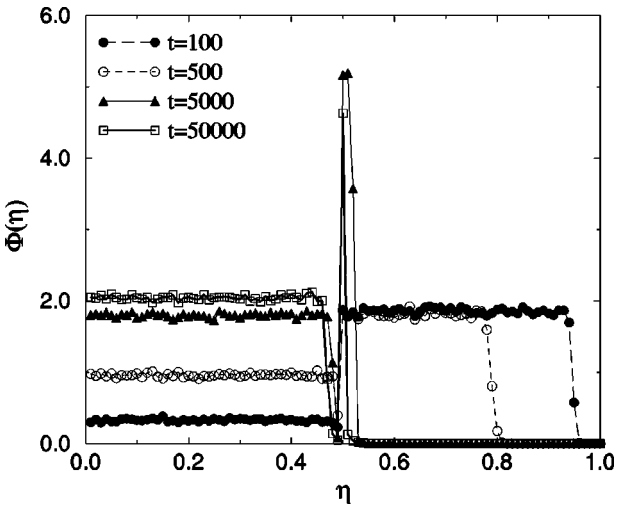

FIG. 12. Histogram $\Phi(\eta)$ (η is an adimensional number) of quenched variables, at different times t, for $p=0.02$.

The roughness exponent accounts for scale free spatial fluctuations in the interface profile. In order to characterize the eventual scale free fluctuations in the dynamical evolution of the system at its asymptotic critical state, that is to say long-range temporal correlations, we have studied the avalanche distribution. An avalanche is defined as a sequence of causally connected elementary growth events. For the class of models with quenched disorder and an extremal dynamics to which our model belongs, the initiator of a critical, scale invariant, avalanche is identified in the critical state by a site with quenched variable $\eta_c^M(p)$ or $\eta_c^S(p)$ (respectively, for an M initiator and for an S initiator). The values of η_c^M and η_c^S

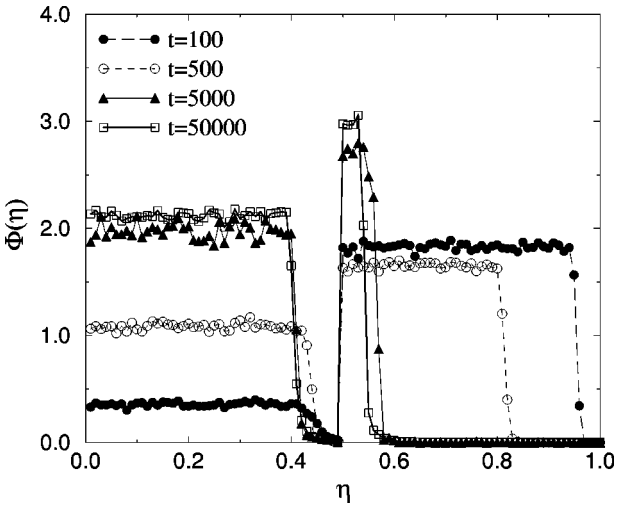

FIG. 13. Histogram $\Phi(\eta)$ of quenched variables, at different times t, for $p=0.2$.

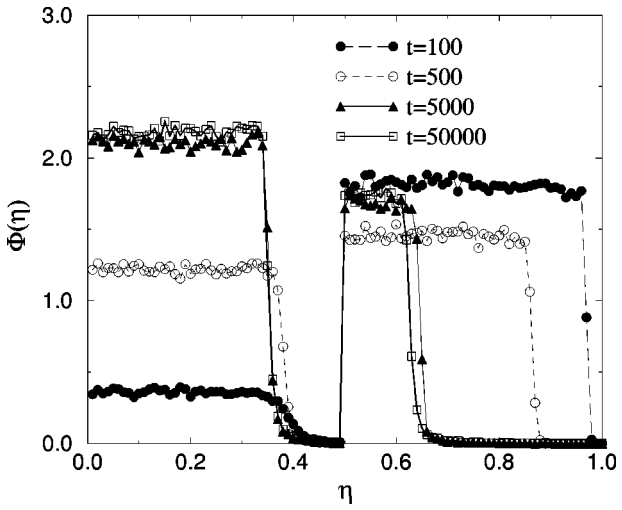

FIG. 14. Histogram $\Phi(\eta)$ (η is an adimensional number) of quenched variables, at different times t, for $p=0.5$.

for different values of p can be obtained by the asymptotic histogram distributions shown in Figs. 11–14. In our case there are two classes of variables, the S and M sites, and two possible initiators for an avalanche. We call the avalanches that start with an S site, S avalanches, and the avalanches that start with an M site, M avalanches. An avalanche lasts when a variable, which has been updated before the growth of the initiator, is selected by the extremal dynamics. The statistics of off-critical avalanches has been shown to have the form [2,20]

$$P^X(s;\eta)=s^{-\tau_X}f_X(|\eta-\eta_c^X|s^{\sigma_X}), \tag{5}$$

where $X=S,M$, and η is the initiator of an X avalanche. This distribution becomes a pure power law for $\eta=\eta_c^X$. In the limit $t\to\infty$ the system self-organizes into the critical state $\eta=\eta_c^X$, and the (normalized) avalanche size distribution becomes

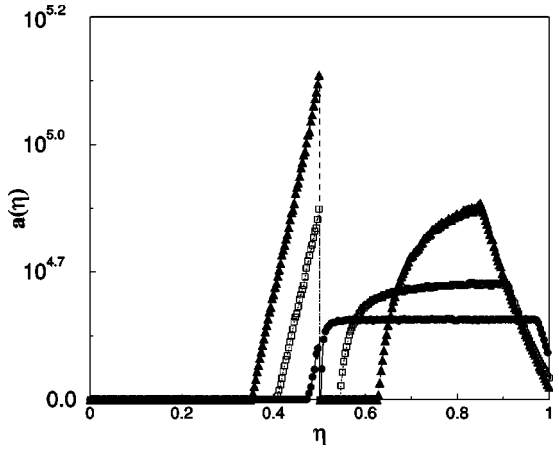

FIG. 15. Asymptotic acceptation (not normalized) profile $a(\eta)$ (η is an adimensional number) for $p=0.02$ (circles), $p=0.2$ (squares), and $p=0.5$ (triangles).

TABLE II. Critical thresholds η_c^S, η_c^M of variables S and M, for different values of p.

p	η_c^S	η_c^M
0.02	0.47(1)	0.50(1)
0.2	0.41(1)	0.54(1)
0.5	0.35(1)	0.63(1)

$$P^X(s;\eta_c^X)=\frac{s^{-\tau^X}}{\sum_{s=1}^{\infty}s^{-\tau^X}}. \tag{6}$$

We have performed a set of about 10^3 realizations of size $L=8192$, lasting each one 2×10^6 time steps, and collected the statistics of S and M avalanches over the last 10^6 time steps, for $p=0.02$, 0.2, and 0.5. These simulations required about two months of CPU time on our computers (a network of DEC alpha machines with clocks going from 266 to 500 MHz), and are at the best of our computation possibilities. To reduce numerical problems connected with the approximation on η_c^M, η_c^S, we used an alternative definition of critical avalanches in models with extremal dynamics, which resides on the causal relation between updated sites inside an avalanche (for details on the definition of critical avalanches see Refs. [21–23]). The results are shown in Figs. 17 and 18. Even after this big computational effort, our numerical results are still a bit noisy. In particular the statistic of S avalanches for $p=0.02$ is really poor. This is due to the fact that for small p values most of sites selected by the dynamics are M sites. Consequently, it is difficult to observe a quite clear power-law behavior for both the S avalanches and M avalanches distributions. We point out that the presence of long-range temporal correlations is not necessary for the model to have self-similar or self-affine spatial properties, as already observed in a different context [25].

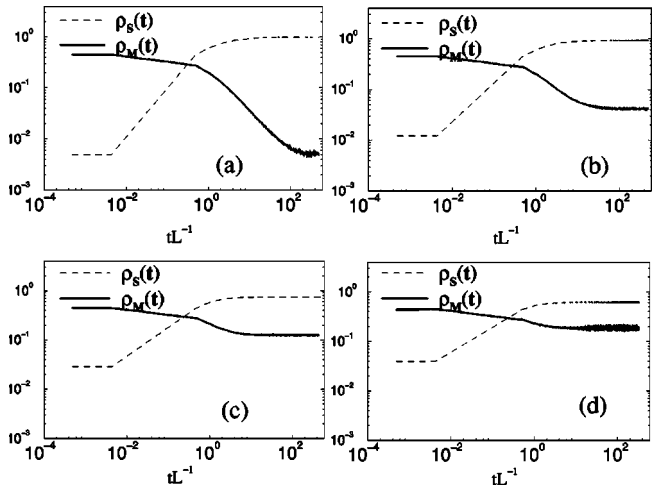

FIG. 16. Time evolution (t is expressed in adimensional computer time units) of the densities ρ_S and ρ_M of sites S and M, respectively, for $p=0.0$ (a), $p=0.02$ (b), $p=0.2$ (c), and $p=0.5$ (d).

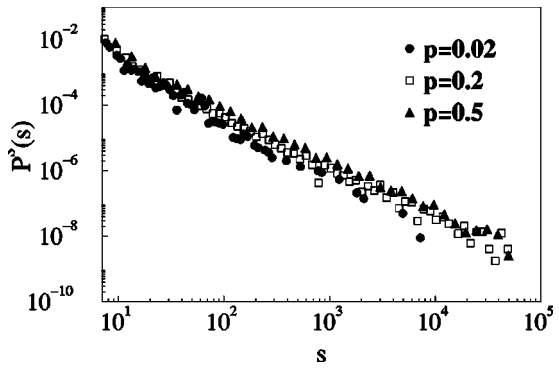

FIG. 17. Binned S avalanches distribution for different values of p.

In order to better establish the critical properties of our model we have measured the power spectrum $S(k)$ of the equilibrium surface. The model studied here is a discretized cellular automaton, which can be thought as a modified version of the Sneppen model for quenched interface growth. The Sneppen model has been shown to be, at least in $1+1$ dimensions, in the same universality class of the continuous Kardar-Parisi-Zhang equation with quenched noise (QKPZ) [24]. It is natural, but not necessarily true, to suppose that for our model, too, it is possible to find a formulation as a continuous growth equation. Given a general growth equation for $h(x,t)$ like

$$\frac{\partial h(x,t)}{\partial t} = A[h(x,t)] + \gamma(x,t), \tag{7}$$

where $A[\ \ldots\ ]$ is an operator acting on $h(x,t)$ and $\gamma(x,t)$ is an uncorrelated quenched noise (the ''temporal'' direction corresponds to the growth direction of the surface), if the operator $A[\ \ldots\ ]$ is linear and local, the equation can be Fourier transformed into

$$i\omega\tilde{h}(k,\omega) = \tilde{A}(k)\tilde{h}(k,\omega) + \tilde{\gamma}(k,\omega), \tag{8}$$

and by introducing the propagator $G(k,\omega)$,

$$\tilde{h}(k,\omega) = G(k,\omega)\tilde{\gamma}(k,\omega), \tag{9}$$

where $G(k,\omega) = [i\omega - \tilde{A}(k)]^{-1}$.

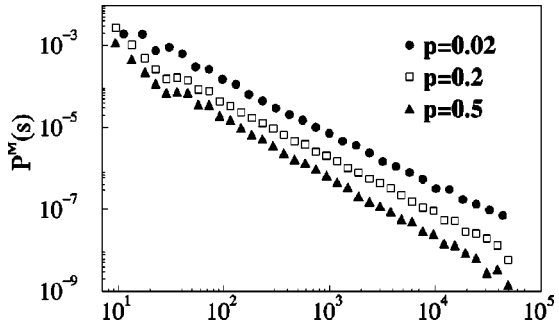

FIG. 18. Binned M avalanches distribution for different values of p.

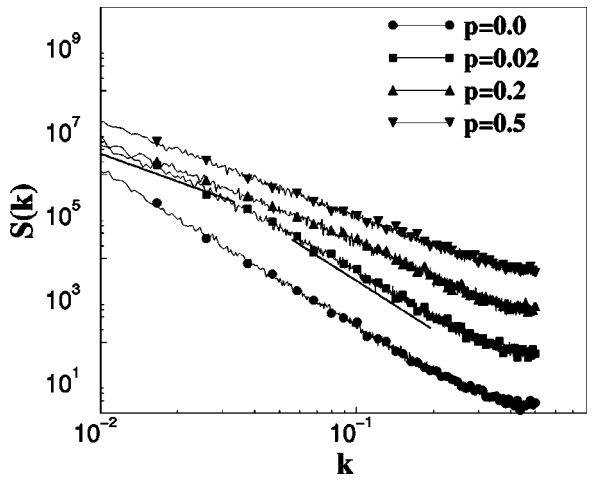

FIG. 19. Power spectrum $S(k)$ (all the quantities are expressed in adimensional units of the computer simulation) of our model for $p=0.0$, 0.02, 0.2, and 0.5 (values referring to, respectively, the plots from bottom to top) and $L=2048$. As a guide for the eye, we report the scaling law for KPZ (dotted line) and QEW (dashed line) universality classes.

The propagator $G(k,\omega)$ of Eq. (7) is related to the power spectrum $S(k)$ of the interface in the asymptotic state. The power spectrum is so defined

$$S(k) = \langle FT[h(x)h(x')]\rangle = \langle|\tilde{h}(k)|^2\rangle, \tag{10}$$

where $FT[\ \ldots\ ]$ is the Fourier-transform operator, the average is over different realizations of the noise, $h(x) = h(x, t=\infty)$, and $\tilde{h}(k)$ is the Fourier transform of $h(x)$. Equation (10) is valid is the case the noise is uncorrelated in space and time, which is the case of our model. The relation between $\tilde{G}(k,\omega)$ and $S(k)$ is the following [3]:

$$\tilde{G}(k,\omega=0)^2 = S(k). \tag{11}$$

Equation (11) tells us that the power spectrum of the interface can give informations on k-dependent part of the propagator $G(k,\omega=0)$ and consequently on the structure of the operator $\tilde{A}(k)$ in Eq. (8). For self-affine surfaces, the power spectrum follows a power-law scaling

$$S(k) \sim k^{-2\delta}, \tag{12}$$

where δ is related to the *global* roughness exponent χ_{glob} through the scaling relation $2\delta = 2\chi_{\mathrm{glob}} + 1$ [3].

Figures 19 and 20 report the behavior of the power spectrum $S(k)$ of the interface profile in the critical state for system sizes $L=2048,8192$ and different values of p.

For large values of k, finite-size effects connected to the discretized nature of the model become relevant and there is a deviation from the power-law behavior. Away from this saturation effect it is evident in this case how $S(k)$ is characterized by a clear crossover between two power-law behaviors. In the low k region $[k < k^* \propto p/(1/2-p) = 1/l^*]$ $S(k)$ scales with an exponent δ_{low} close to 1 [actually

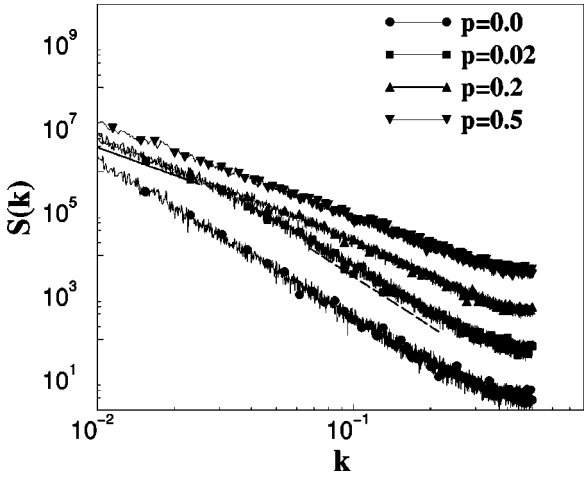

FIG. 20. Power spectrum $S(k)$ (all quantities are expressed in adimensional units of the computer simulation) of our model for $p=0.0$, 0.02, 0.2, and 0.5 (values referring to, respectively, the plots from bottom to top) and $L=8192$. As a guide for the eye, we report the scaling law for KPZ (dotted line) and QEW (dashed line) universality classes.

1.07(3)] for all values of p. The QKPZ (Sneppen B model) universality class is characterized by a global roughness exponent [coinciding with the local exponent we have measured through $W^2(l)$] $\chi_{\mathrm{glob}}=\chi=0.63$, giving $\delta=1.13$, quite near to what we find. For intermediate values of k [$k>k^* \propto p/(1/2-p)=1/l^*$] one gets an exponent δ_{mid} quite near to the value 1.7 (we find values between 1.7 and 1.86) which corresponds to the quenched-Edwards-Wilkinson (QEW) universality class ($\chi_{\mathrm{glob}}\sim 1.2$ [3]), independently of the value of p. We point out that the QEW model is super rough with a global roughness exponent $\chi_{\mathrm{glob}}\sim 1.2$, and a local exponent $\chi=1.0$ [the one we measured through $W^2(l)$]. For p near 0.5 the intermediate k region is very small, and it is difficult to distinguish it from the saturation region. The same happens when one tries to fit the low k region for p close to zero. If $p=0.0$ or $=0.5$, no crossover effect is observed, since these two values of p correspond to the ''pure'' QEW and KPZ universality classes, respectively.

From these results we have a confirmation that the model *does not exhibit nonuniversal critical properties*. The apparent nonuniversal roughness exponent is the consequence of a crossover effect, tuned by the parameter p. The fact that this crossover effect is difficult to observe when studying the scaling of the mean-square width $W^2(l)$ of the sample, could explain the discrepancy between the experimental findings available in the literature.

IV. CONCLUSIONS

In this paper we have introduced a model for surface roughening whose main peculiarity is that of taking explicitly into account the anisotropy of the growth process by means of a tunable phenomenological parameter p, which introduces local, i.e., dependent on the local environment, dynamical rules in the growth. The simple introduction of just one anisotropy parameter p is far from being able to capture *all* the characteristics of etching processes, and in general of surface roughening experiments. In etching experiments, for example, transport phenomena in the solution are likely to be important and both concentration and agitation have strong effects on transport. Nevertheless, our model captures at least some basic elements of the relationship between anisotropy and the apparent nonuniversality observed experimentally in etching processes. Moreover, the general requirement of a microscopic dynamical rule depending on the local environment could be a key element in the apparently observed nonuniversality in kinetic roughening phenomena.

As a main outcome, the model exhibits a crossover behavior in its critical properties. For each value of the anisotropy factor p the system reaches a critical stationary state, with a characteristic length separating a KPZ-like (Sneppen B model) behavior from a QEW-like (Sneppen A model) behavior. The crossover from one scaling behavior to the other is tuned by the anisotropy parameter p. If one looks at the scaling of $W^2(l)$, the crossover effect cannot be easily discovered, and the system seems to have a nonuniversal roughness exponent. A careful analysis of the power spectrum $S(k)$, however, shows a clear crossover effect. These results can probably help to explain the relevant discrepancies among experimental results [10–12]. We believe that this behavior is the outcome of the complex interplay between the global dynamics, which selects at each time step the weakest site and the anisotropy effect that takes into account local constraints in the growth.

It is worthwhile to stress how our model suggests the possibility of several analytical approaches, from the treatment of the problem in terms of a continuous stochastic dynamical equation, to the single site mean-field approach [26], or to the application of a method recently proposed for dynamical models driven by an extremal dynamics [21–23,27]. Particularly promising, in this respect, is a recently proposed nonperturbative renormalization-group approach [28], which allows one to study self-affine problems.

ACKNOWLEDGMENT

The author acknowledges financial support under the European network Project No. FMRXCT980183.

[1] P. Bak, C. Tang, and K. Wiesenfeld, Phys. Rev. Lett. **59**, 381 (1987).

[2] M. Paczuski, S. Maslov, and P. Bak, Phys. Rev. E **53**, 414 (1996).

[3] See, for example, the exhaustive review, T. Halpin-Healy and Y.-C. Zhang, Phys. Rep. **254**, 215 (1995), and references therein.

[4] G.S. Bales, A.C. Redfield, and A. Zangwill, Phys. Rev. Lett. **62**, 776 (1989).

[5] G.L.M.K.S. Kahanda, X.Q. Zou, R. Farrell, and P.-Z. Wong,

Phys. Rev. Lett. **68**, 3741 (1992).
[6] M. Kardar, G. Parisi, and Y.-C. Zhang, Phys. Rev. Lett. **56**, 889 (1986).
[7] K. Sneppen, Phys. Rev. Lett. **69**, 3539 (1992).
[8] L.H. Tang and H. Leschhorn, Phys. Rev. A **45**, R8309 (1992); T. Nattermann, S. Stepanow, L.H. Tang, and H. Leshhorn, J. Phys. II **2**, 1483 (1992).
[9] B. Sapoval, S.B. Santra, and Ph. Barboux, Europhys. Lett. **41**, 297 (1998); A. Gabrielli, A. Baldassarri, and B. Sapoval, preprint, cond-mat/0002298.
[10] J. Zhang, Y.-C. Zhang, P. Alstrom, and M.T. Levinsen, Physica A **189**, 383 (1992).
[11] M.A. Rubio, C.A. Edwards, A. Dougherty, and J.P. Gollub, Phys. Rev. Lett. **63**, 1685 (1989).
[12] V.K. Horvath, F. Family, and T. Vicsek, Phys. Rev. Lett. **65**, 1388 (1990).
[13] R. Cafiero, V. Loreto, and P. Prosini, Europhys. Lett. **42**, 389 (1998).
[14] E. Yablonovitch and G.D. Cody, IEEE Trans. Electron Devices **ED-29**, 300 (1982).
[15] H. Seidel, L. Csepregi, A. Henberger, and H. Boumgartel, J. Electrochem. Soc. **137**, 3612 (1990).
[16] M. Elwenspock, J. Electrochem. Soc. **140**, 2075 (1993).
[17] P. Allongue, V. Costa-Kieling, and H. Gerischer, J. Electrochem. Soc. **140**, 1009 (1993); **140**, 1018 (1993).
[18] V. Loreto, A. Vespignani, and S. Zapperi, J. Phys. A **29**, 2981 (1996).
[19] J.M. Kim and J.M. Kosterlitz, Phys. Rev. Lett. **62**, 2289 (1989).
[20] S. Maslov, Phys. Rev. Lett. **74**, 562 (1995).
[21] M. Marsili, Europhys. Lett. **28**, 385 (1994).
[22] A. Gabrielli, R. Cafiero, M. Marsili, and L. Pietronero, Europhys. Lett. **38**, 491 (1997).
[23] R. Cafiero, A. Gabrielli, M. Marsili, and L. Pietronero, Phys. Rev. E **54**, 1406 (1996).
[24] G. Parisi, Europhys. Lett. **17**, 673 (1992).
[25] A. Gabrielli, R. Cafiero, and G. Caldarelli, Europhys. Lett. **45**, 13 (1999).
[26] R. Dickman, J. Stat. Phys. **55**, 997 (1989).
[27] M. Marsili, J. Stat. Phys. **77**, 733 (1994); A. Gabrielli, M. Marsili, R. Cafiero, and L. Pietronero, *ibid.* **84**, 889 (1996).
[28] C. Castellano, M. Marsili, and L. Pietronero, Phys. Rev. Lett. **80**, 3527 (1998).